Journal of Aviation and Aerospace Technology, Vol. 1 No. 1 (2019) p. 1-13

JAAT

FAZ Publishing

Journal of Aviation and Aerospace Technology

Journal homepage : www.fazpublishing.com/jaat

e-ISSN : 2682-7433

Development of Vertical Take Off High Payload Drone Unmanned Aerial Vehicle

Saidah Idrus[1], Mohd Fadhli Zulkafli[2,*]

[1]Faculty of Mechanical and Manufacturing Engineering
Universiti Tun Hussein Onn Malaysia, 86400 Parit Raja, Johor, MALAYSIA.

Received 20 November 2018;
Accepted 10 January 2019;
Available online 5 March 2019

Abstract: Unmanned Aerial Vehicle (UAV) is a semi or fully autonomous aircraft that can fly without direct control or able to remotely controlled from ground control station. Even though UAVs were widely used for military operation at first, its use is rapidly extending to commercial, scientific, recreational, agricultural and other applications such as peacekeeping and surveillance, product deliveries and policing. For current available UAV that uses battery as source of power, maximum payload that can be carried is 30 kg. This small range of payload can be increased to ease and extending UAVs' application for improved and effective working conditions. Hence, the proposed design of UAV for this study is a quadcopter applying coaxial propulsion configuration. The objective for this thesis is to investigate the design requirements for high payload drone, specifically 200 kg of payload. Concept certification requirements developed by Peak in the Delta (PID) Unmanned Aerial System (UAS) Innovation Project titled as Certification Specification - Light Unmanned Multi Rotor Systems (CS-LUMRS) was used for comparison with the proposed design of UAV. Carry on to the second and third objective where the aerodynamics properties and the performance by high payload drone was studied. This study uses Solidworks 2016 Flow Simulation to simulate the fluid flow across the designated propeller to find the relation between thrust generated with the rotational speed configured on the propeller. Similarly, this simulation also provide aerodynamic properties such as drag forces formed at the back of the drone as it moves across the fluid flow. Above all, the proposed design of high payload drone does able to take off with maximum weight of payload by means of 200 kg and hover where increment in rotational speed will results in rise in generation of thrust by the propellers.

Keywords: Unmanned Aerial Vehicle, high payload drone, flow simulation

1. Introduction

Unmanned aerial vehicle (UAV) is also known as drone is an aircraft which have no on board human pilot. Previously, UAVs are famously used for military applications such as aerial reconnaissance, carrying out surveillance mission and organizing weapons [1].

Over the years, with significant recognition for the role of drones, drones are now developed extensively for civil applications. Currently, there are companies that are conducting research to develop a drone that can even transport people. "One man drone" project developed by the Dutch and Ehang 184 manufactured by company from China and has been launched in Dubai [2]. Both of the developed UAV are utilizing electric propulsion. These ideas are developed alongside with the concept of urban mobility which urban air transportation will use three-dimensional airspace to alleviate transportation congestion on the ground [3].

Due to its heavy targeting payload, a size of a human, quadcopter or quadrotor configuration is used as well as coaxial propulsion for minimizing the power consumption however enabling optimum thrust to be lifted.

Several researches were done regarding coaxial propulsion. Experimental and analytical studies summarize by Coleman [4] where visualization of flow through single, tandem and coaxial arrangement were done. It was found that coaxial rotor required 5% less power compared to single rotor in forward flight by experimental data. Another study [5] also finalized that coaxial system demands less induced power than the conventional system, single rotor. The axial convection rate at the tip vortices for the top rotor is higher than for the tip vortices of the same rotor operating in isolation. Another advantages of coaxial propulsion system is coaxial configuration has more solid structure than a single rotor because it does not require to mount a rear shaft longer than the main rotor's blade-swept radius in the airframe. This instance results in reducing of coaxial-rotor size by 35-40% as compared with the single-rotor one [6]. This paper also states

**Corresponding author: fadhli@uthm.edu.my*

that from coaxial propulsion, it uses two contra rotating rotors to compensate each other's torque that they apply to the vehicle fuselage as they rotate.

For this study, the proposed design of UAV is classified into a four-rotor coaxial configuration which also known as quadcopter or quadrotor. Using of four rotor denote that the lift generated are from four sources which reducing the needs of one single rotor to rotate and produce high revolutions per minute (RPM). With contra-rotating coaxial rotor configuration, overall rotor diameter can be reduced since the thrust vector from each rotor is directed vertically upward, and so each rotor provides a maximum contribution to vertical thrust to overcome vehicle weight.

The designated quadcopter is tend to carry a passenger with maximum payload of 200 kilograms. With this high payload, the most important component in effecting the performance of the quadcopter is the propulsion system as it influenced approximately 90% of the power consumption of the rotors [7]. Propulsion system for this quadcopter should be efficient and proper with the mass of the vehicle and its payload to gain long flight time.

The study of this paper utilized Solidworks 2016 Flow Simulation to investigate the fluid flow across the UAV, thrust generation and formation of drag forces. Also, the proposed designation of drone shall be compared with authorized design requirement certification to meet the airworthiness code.

2.0 Design requirement

The proposed design was compared in terms of airworthiness code, regulations and certification specification. The comparison was made by distinguishing between the proposed design of UAV with the standard published by the Peaks in the Delta (PID) Unmanned Aircraft System (UAS) Innovation Project. The objective of this project is enabling the qualification of multi rotor Remotely Piloted Aircraft System (RPAS) for less limited, urban or congested area of operations by establishing a concept of Certification Specification for Light Unmanned Multi Rotor Systems (CS-LUMRS).

3.0 Flow Simulation

In this study, two different features of flow simulation were conducted. Solidworks Flow Simulation enables to simply simulate liquid and gas flows through and around the designs rapidly with the purpose of calculating performance and capabilities of the proposed design.

3.1 Pre-processing for Thrust Generation by Coaxial Propulsion

Coaxial propulsion was configured by using a simple assembly tool to setup as shown in Fig 1. The angle of attack for the two propellers was the primary feature taken into attention during the assembly with the aim of producing counter rotating propulsion system.

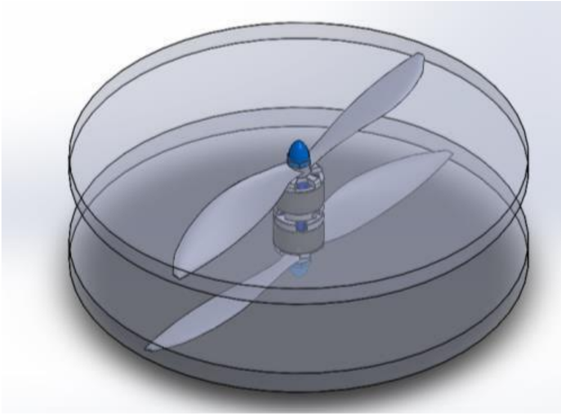

Fig 1- Coaxial propulsion configuration

Next, the parameters were inserted into the wizard dialog box as shown in Table 1.

Table 1- General settings of Flow Simulation for coaxial propulsion

Unit System	SI
Analysis Type	External • Exclude cavities without flow condition • Exclude internal space Physical feature • Rotation Reference • Y-axis
Fluid	Gases • Air Flow Characteristic • Laminar and turbulent
Wall Condition	Default • Adiabatic wall •0 micrometer of roughness
Parameter	Pressure : 101 325 Pa Temperature : 293.20 K

(a) Computational Domain

Once completing placed in all the required parameters into the dialog box, a transparent enclosure was automatically built in. This enclosure is known as computational domain. The computational domain is the rectangular parallelpiped section where the 3D flow analysis calculations were executed. The computational domain's boundary planes are automatically distanced from the model as the external flow type of analysis is to be done.

Published by FAZ Publishing
http://www.fazpublishing.com/jaat

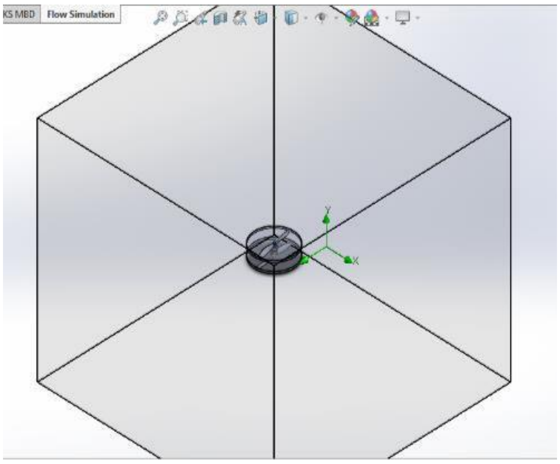

Fig 2- Computational domain enclosing the coaxial propulsion configuration

(b) Local Rotating Region

By creating local rotating region, only propellers out of entire components in the assembly is the fragment of the rotating region. Rotating region generally assumes that a model is entirely symmetric about the rotating axis and all the components within the computational domain are rotating at the speed specified on the rotating reference frame.

Thus, the constraints were inserted into the wizard dialog box. Positive value of angular velocity indicates the counter clockwise direction meanwhile negative value of angular velocity specifies clockwise direction of rotation as shown in Figure 3.

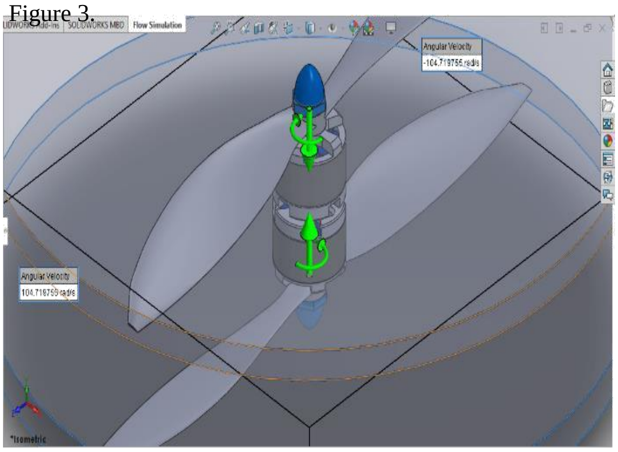

Fig 3- Direction of rotation

(c) Surface Goals

The foremost purpose of Goals is to outline the vital design objectives of the simulation. As surface goal is a physical parameter calculated on the selected surfaces, all propellers' surfaces were chosen.

The goal for this simulation is merely to find the thrust that can be generated by the coaxial propulsion with specified angular velocity. Thus, Force (Y) which indicating forces generated in y-axis, was selected in wizard dialog box as goal to be calculated.

(d) Meshing

Meshing is a distinct representation of the geometry which involved in the problem and to be solved computationally. Fundamentally, in order to analyse fluid flows, flow domains are split into smaller subdomains. The governing equations are then discretized and solved inside each of these subdomains.

In Solidworks Flow Simulation, this software offers automated meshing process by default unless manual type of meshing is picked. Under automatic meshing, level of initial mesh which governs the number of basic mesh cells can be varied from scale 1 to 7. Higher scale of meshing results in higher number of mesh cells. And in this study, level of initial mesh on scale 5 and refinement level at scale of 3 was selected.

Besides global meshing, local mesh also were specified at scale of 4. Local mesh permits to specify an initial mesh in a local region of the computational domain to improve the resolution of the model specific geometry and flow peculiarities within this region, which cannot be well-resolved under global initial mesh settings. Consequently, there was single local mesh done. The components selection for the local mesh was the propeller region plus rotating region. These control setting of meshes is significant because it determines the quality of the mesh which then leads to the exactness of the flow simulation calculated.

3.2 Pre-processing for Forward Moving High Payload Drone

The assembly of the component used simple assembly tools of mates. This configuration was setup to study the drag force created as the drone is hovered in the air with maximum velocity of 60 km/h.

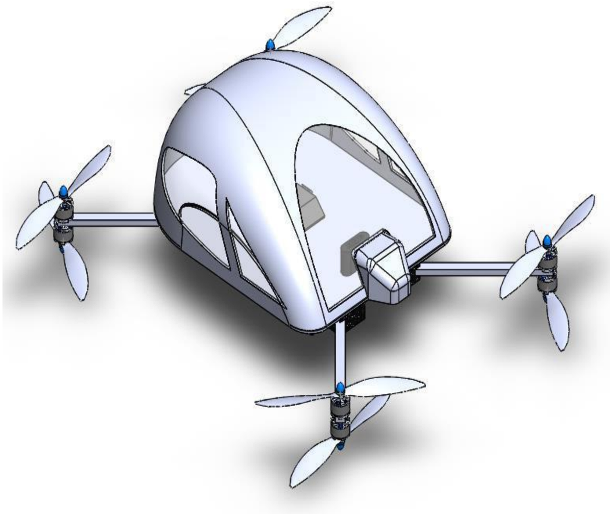

Fig 4-Model of High Payload Drone

The setup for this study is relatively different compared to previous study. The setup for this study is as presented in Table 2:

Table 2- Volume of Bio-oil harvested

Unit System	SI
Analysis Type	External • Exclude cavities without flow condition • Exclude internal space Reference • Y-axis
Fluid	Gases • Air Flow Characteristic • Laminar and turbulent
Wall Condition	Default • Adiabatic wall •0 micrometer of roughness
Initial	Thermodynamic Parameter • Pressure : 101 325 Pa • Temperature: 293.20 K Velocity Parameter • Defined by Aerodynamics angle • Velocity : 16.667 m/s • Longitudinal plane: XY • Longitudinal axis : X • Angle of attack: 10°,15°,20°,25° and 30°

(a) Computational Domain

Since the flow analysis specified as external analysis, the computational domain was automatically constructed by default. However, the domain was adjusted, where the computational domain on the behind of the drone was fairly larger compared to the front domain of the drone. This arrangement as in was made for the reason that this simulation is focusing on drag forces at the back of the drone and to display continuous air velocity trajectory after air particles encountered the drone.

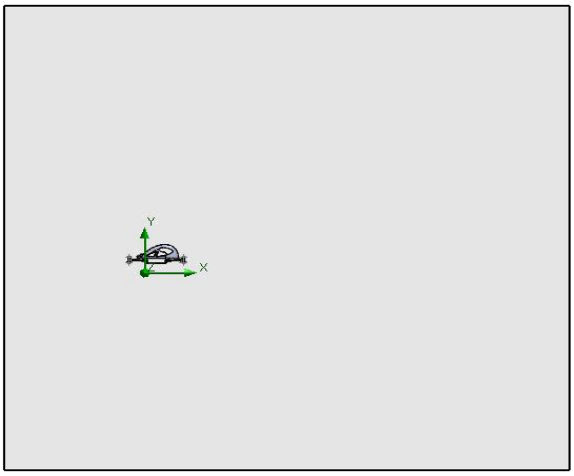

Fig 5-Computational domain of the model

(b) Global Goal

Differ from previous study which Surface Goal was applied, this task used Global Goal where physical parameters are to be calculated in the entire computational domain. With the target for this simulation is to achieve drag force created in forward moving by the model, the Force (X) in the wizard dialog box of global goal is selected.

(c) Meshing

The size of global mesh cells and local mesh cells for this simulation can be controlled from the dialog box as the setting was set at 5 and display refinement level was set at 3. As for local mesh setting, all faces of components were selected hence the meshing of the model was set at scale of 3.

3.3 Calculation Control

The solver will conduct the analysis alongside with mesh generation operation. In Calculation Control dialog box, under Finishing Calculation tab, Goals Convergence finishing condition was selected.

If there are no goals specified or no goals are taken into account as finishing conditions, the Flow Simulation internal convergence criteria will be used to finish the calculation. With this condition, the calculation finishes immediately after the specified goals have converged. As the solver is finish, value produced for selected goals previously will be displayed.

3.4 Post-processor

This is the last step for Solidworks Flow Simulation process. During this phase, all results will be produced visually and numerically. The data attained can be visualized in various means such as contours, isolines, streamlines, vector and mesh for all parameters. Solidworks post-processor too offers animation and flow trajectories for the data achieved.

4.0 Results and Discussion

4.1 Comparison in Design of High Payload Drone

Generally, the requirements made are applicable for light unmanned multi-rotor systems, maximum take-off mass of 150kg to be specific.

Table 3- General requirements

No	General Requirements
1	Less limited, urban/congested area
2	Land with no excessive vertical acceleration
3	Flown below 120 m (400ft)
4	No further than 500 m from pilot-in-command (PIC)
5	Minimum horizontal distance of 150m from public and buildings
6	Aircraft shall be able to perform one or more evasive manoeuvre(s) to ensure sufficient separation with other aircraft.

Published by FAZ Publishing
http://www.fazpublishing.com/jaat

7	Aircraft shall be free from excessive vibrations under any operational speed and power condition.
8	Factor of safety of 1.5 shall be used
9	A limit manoeuvring load factor ranging from a positive limit of 3.5 to a negative limit of -1.0
10	Motor mount and adjacent fuselage structure shall be designed to withstand the loads occurring
11	Failure detection apparatus will include propulsion system health monitoring of motor critical data (for example temperature and RPM).
12	The addition of the rotor and the rotor drive system to the engines shall not subject the principal rotating parts of the engine to excessive vibrations or vibration stresses.

Table 4- Comparison of the proposed design with airworthiness certification

Certification Specification	Proposed Design
Class 1 : Max take-off 150kg	Mass of drone + Payload : 589 kg
Max speed: 70knots (129.64 km/h)	Operational speed : 60 km/h
Empty mass (aircraft mass without payload) : 389 kg	Mass of the design : 389 kg
Aircraft shall be able to continue its flight with one rotor inoperative	Series circuit of battery system applied. Either only top/bottom inoperative. Drone stability can be maintained.
Wind velocity of not less than operational wind velocity.	Operational wind velocity in hovering : 16.667 m/s
Motors shall be separated from each other	Each motor placed in each motor hub
Aircraft shall be able to maintain a stable flight without pilot input.	Passengers are treated as static load
Limit loads (the maximum loads to be expected in service)	200 kg
Ultimate loads (limit loads multiplied by prescribed factors of safety)	200 kg x 1.5 = 300 kg
Maximum take-off mass with a rotor lift, which shall not exceed two-thirds of the design maximum mass;	2/3 design maximum mass : 389 x 2/3 = 259.33 kg Max take off mass (current design) : 589 kg
The suitability and durability of materials: I. Established on the basis of experience or tests. II. Meet industrial specifications that	Material properties setup using general mechanical properties of the materials
Incorporate a locking device. No self-locking nut shall be used on any bolt subject to rotation	The design does not include fasteners to all part of components
The effects of temperature of materials on allowable stresses	Studies on design materials yet to be tested
Shall be enough clearance between the propellers and other parts of the structure	Clearance between propeller and body of drone : 11.29 cm front side 3.96 cm back side
Landing gear unit shall be tested in the attitude simulating the landing condition	Have yet to be conducted

The proposed design of high payload drone is yet to fully satisfy the airworthiness certification. The biggest contrast can be seen is in terms of material properties. The material selection done was by taking the broad advantages of the material and based on its widespread usage in industrial aircraft applications.

4.2 Computational Fluid Dynamics

(a) Thrust Generation

According from the pressure contour, the pressure difference produced from the propeller can be observed. Theoretically, higher rotational speed applied onto propeller

Published by FAZ Publishing
http://www.fazpublishing.com/jaat

will formed lower air pressure thus create more lift force. Consequently, the capability for the high payload drone to be lifted can be resolved by observing the pressure contour formed and calculating the pressure difference.

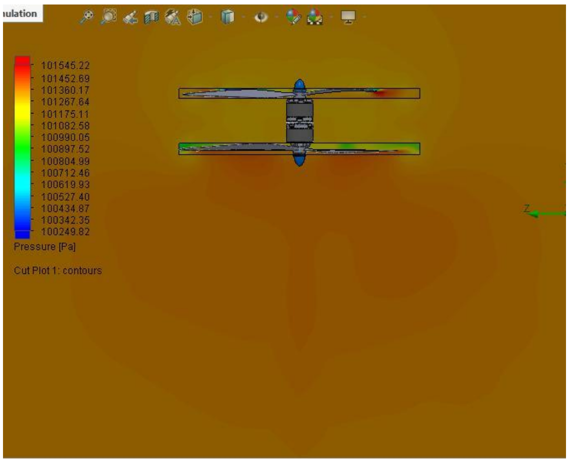

Fig-(a) Rotational speed 1000 RPM

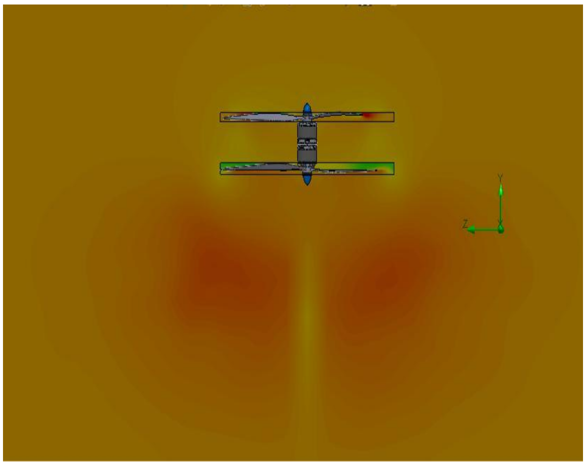

Fig-(b) Rotational speed 2000 RPM

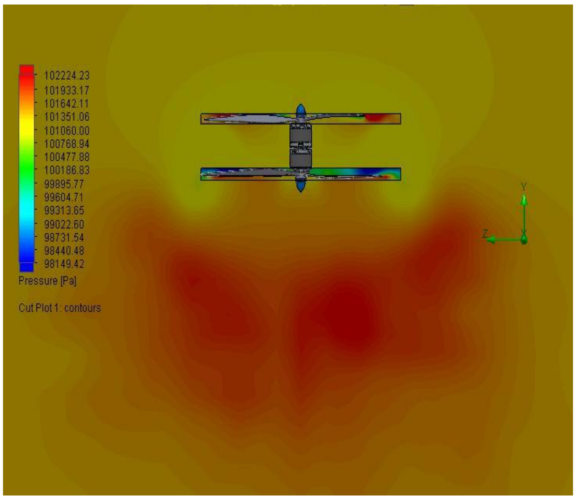

Fig-(c) Rotational speed 3000 RPM

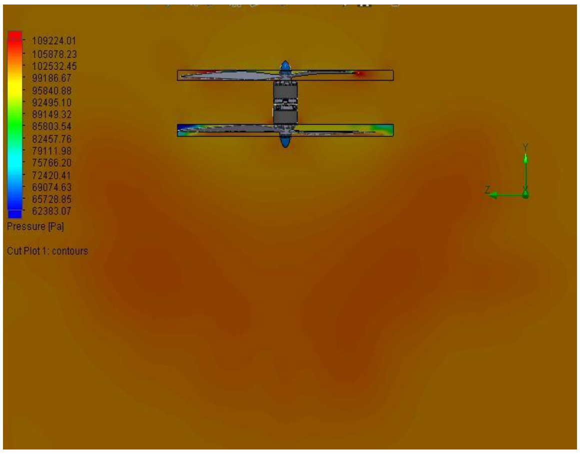

Fig-(d) Rotational speed 4000 RPM

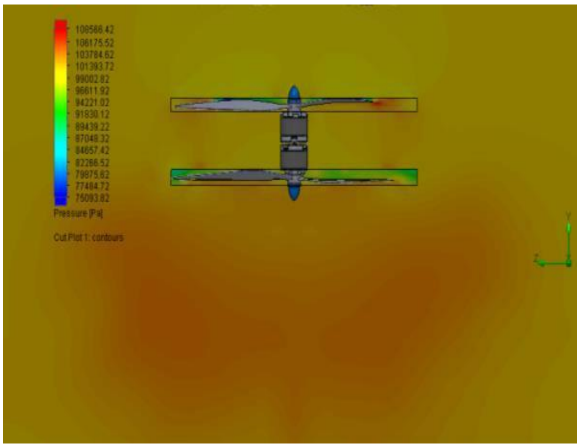

Fig-(e) Rotational speed 5000 RPM

Fig 6-Pressure distribution around the propeller at different rotational speed

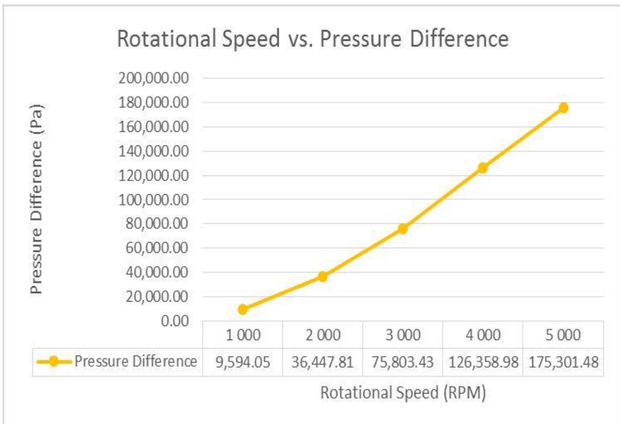

Fig 7-Pressure difference created at different rotational speed

From graph in Figure 7, it is clear that as the rotational speed of the propeller increases, the pressure difference also increase.

Published by FAZ Publishing
http://www.fazpublishing.com/jaat

By the velocity contour, the air velocity passing through propeller can be perceived. Ideally, higher rotational speed applied onto propeller will cause higher velocity of the propeller, alongside with increases in air velocity passing through.

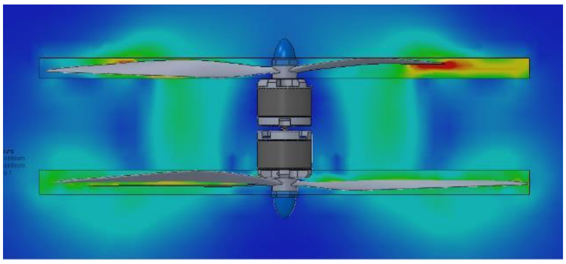

Fig-(a) Rotational speed 1000 RPM

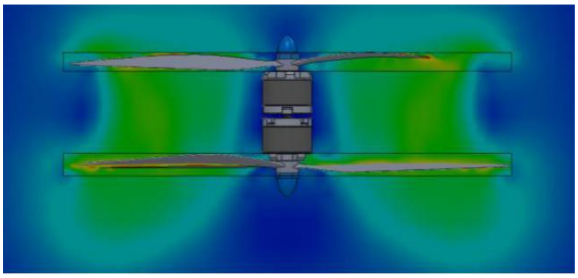

Fig-(b) Rotational speed 2000 RPM

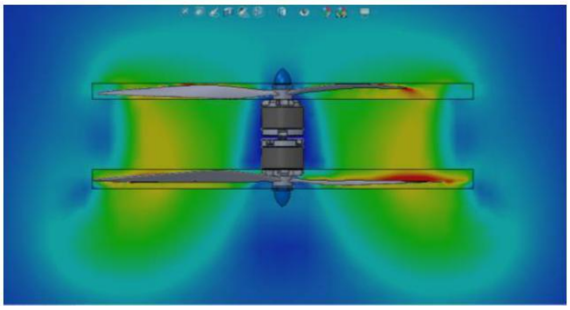

Fig-(c) Rotational speed 3000 RPM

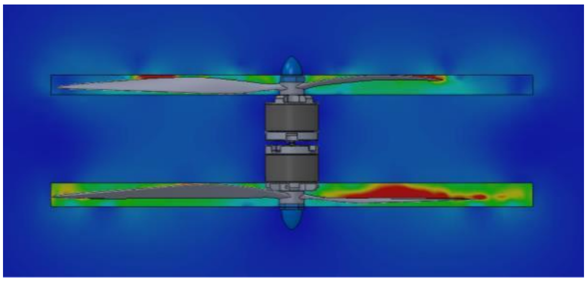

Fig-(d) Rotational speed 4000 RPM

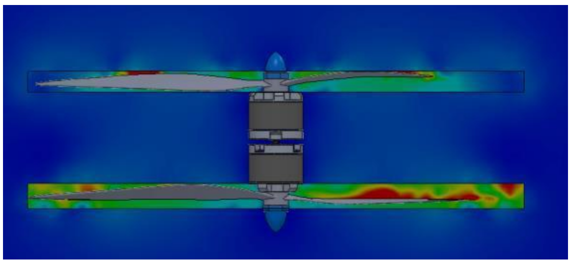

Fig-(e) Rotational speed 5000 RPM

Fig 8-Velocity distribution around the propeller at different rotational speed

Based from Figure 8, it can be seen clearly the air velocity at the tip of the propeller possessed the highest value of velocity for every rotational speed configured.

This is because, from the formula of angular velocity, in Equation 4-1,

$$\omega = \frac{\theta}{t} \quad \textbf{(4-1)}$$

where

$$\theta = \frac{s}{r} \quad \textbf{(4-2)}$$

$$\omega = \frac{s}{rt} \quad \textbf{(4-3)}$$

whereas is the distance travelled to complete 1 revolution and is the length from pivot point, which in this case is the diameter of the propeller and the radius of the propeller respectively.

Therefore, increase in diameter of the propeller relative to the increment of propeller's radius results in high air velocity at the tip of the propeller compared to the other section.

Also by referring to Figure 8, it is noticeable that the increment in rotational speed results in rises in minimum and maximum value of air velocity. This can be validated theoretically where

Velocity at the tip of propeller

$$V_{tip} = \omega r \quad \textbf{(4-4)}$$

Hence, as the radius of the propeller is kept constant, increase in rotational speed of the propeller leads to increment in velocity of air at the tip of the propeller.

Correlated to the pressure difference and velocity distribution attained, values of thrust produced as rotational speed configured changes can be observed evidently by plotting a graph from the data in Table 5.

Table 5- Result data obtained from flow simulation

Rotational Speed (*RPM*)	Thrust (*N*)
1000	265.74
2000	741.05
3000	1424.15
4000	4843.26
5000	6194.17

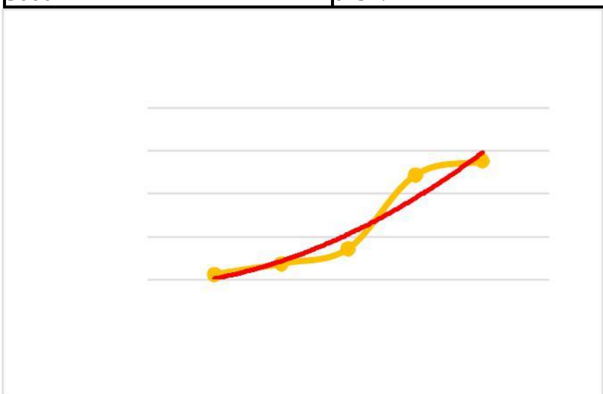

Published by FAZ Publishing
http://www.fazpublishing.com/jaat

Fig 9-Thrust generated at different rotational speed

From the graph in Figure 9, it is obvious that the thrust produced is effected by rotational speed.

The highest thrust produced is 6,194.174 N as the setup of rotational speed was 5,000 RPM which producing the highest pressure difference, 5,520.546 Pa. From the result, it can be said that the duration for the drone to take off is faster as the rotational speed of propeller increases. This instance is due to the reason that as per rotational speed of propeller increases, it causing the air velocity on the top surface of the propeller to be faster. Higher velocity of air molecules create lower air pressure. Eventually, pressure difference formed relative to the air velocity enabling the drone generate thrust.

Lift coefficient is a value that aerodynamicists practice to model all of the difficult dependencies of shape, inclination, and certain flow conditions on lift. The equation is merely a rearrangement of the thrust equation to be solved for the lift coefficient in terms of other variables.

By rearranging to get C_L,

where is the thrust generated, is the average air density around the propeller, is the reference area and is the tip velocity of the propeller. In order to obtain the parameters have to be calculated first. Value of thrust, , and air density, can be directly achieved from the flow simulation result while reference area, with radius of the propeller is constant at 0.7m. Left behind is the value of tip velocity, that can be calculated by multiplying rotational speed, with the radius of the propeller, .

$$\boldsymbol{Vtip = \omega R} \qquad (\mathbf{4-7})$$

Thus from Equation 4-5 and Equation 4-6, data can be tabulated as follow:

Table 6- Tabulated data for CL

Rotational Speed (RPM)	Thrust (N)	Density ($kg/\ m3$)	Tip Velocity (m/s)	CL
1000	265.74	1.20	73.30	0.0535
2000	741.05	1.18	146.61	0.0380
3000	1424.15	1.14	219.91	0.0336
4000	4843.26	1.10	293.22	0.0665
5000	6194.17	1.08	366.52	0.0555

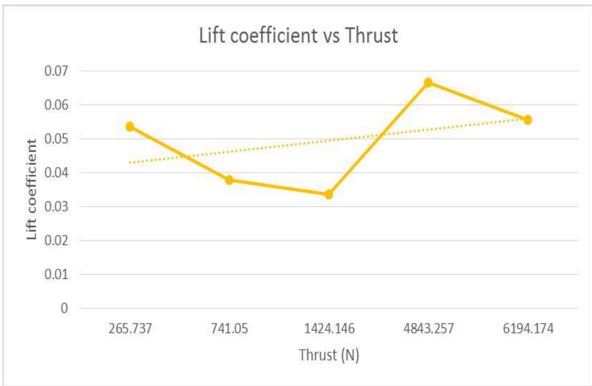

Fig 10-Lift coefficient against thrust generated

From the graph in Figure 10, although the exact value of is fluctuating however the trend line for the graph is linearly increased. The fluctuation occurred may cause by the uneven increment of thrust formed by the propeller and also the tip velocity of propeller.

$$T = \frac{C_L V_{tip}^{\ 2} \rho A}{2} \qquad \textbf{(4-5)}$$

4.3 Performance of the UAV

$$C_L = \frac{2T}{\rho A V_{tip}^{\ 2}} \qquad \textbf{(4-6)}$$

(a) Rotor Efficiency

In order to study regarding the performance of the propeller, efficiency is the main factor should be considered to categorise the performance. Propeller's efficiency, is determined by

$$\eta = \frac{Output\ power, P_{out}}{Input\ power, P_{in}} \times 100\% \qquad \textbf{(4-8)}$$

where input power, have been specified to be 135 kW. In order to obtain the output power, by the propeller, the equation is as follow:

$$Pout = QVtip \qquad (\mathbf{4-9})$$

where Q (Nm) is the torque exerted from the propeller. Values of torque, Q can directly be taken from the simulation result. Hence, tabularization of data is as follows:

Table 7- Power efficiency for top propeller

RPM	Torque, $Qtop$ (Nm)	Output Power, $Pout$ (W)	Efficiency, ηtop
1000	12.37	906.59	0.67
2000	36.89	5,408.65	4.01
3000	87.35	19,209.93	14.23
4000	234.46	68,746.38	50.92

Published by FAZ Publishing
http://www.fazpublishing.com/jaat

5000	350.36	128,414.38	95.12

Table 8-Power efficiency for bottom propeller

RPM	Torque, $Qdown\ (Nm)$	Output Power, $Pdown$ (W)	Efficiency, $\eta down$
1000	-10.63	779.15	0.58
2000	-38.20	5,600.41	4.15
3000	-82.82	18,213.07	13.49
4000	-239.90	70,343.53	52.11
5000	-356.02	130,488.88	96.66

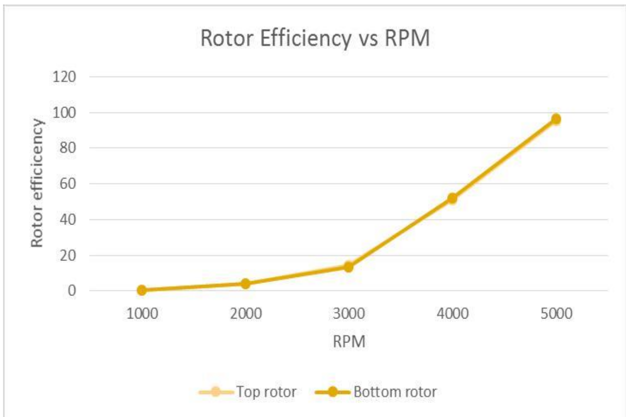

Fig 11- Efficiency of rotor

Because contra-rotating propulsion system was designed, negative value of torque for the bottom propeller based on Table 7 and Table 8 indicates the rotation direction for the propeller that is clockwise direction as positive torque specifies counter-clockwise direction.

The presented data shows that as the rotational for the propeller increases, the output power needed correspondingly increases. These data carries on to the ratio of supplied power, with the intention of attaining the efficiency of rotor with. Hence the tabulated data were plotted into a graph and it is evidently display that rotor efficiency increases as the rotational speed of propeller increases.

With the intention of identifying the capability of drone to be lifted by the rotational speed configured, resultant forces that acting onto the drone shall be resolved.

According to Newton's second law of motion, the vector sum of the forces, on an object is equal to the mass, of that object multiplied by the acceleration of that object as shown in Equation 4-10.

$$\Sigma F = ma \qquad (\mathbf{4-10})$$

By applying the equation onto the drone and targeting the drone to be hovered in the air, where zero acceleration occurs, thrust generated by the propeller must be equal to the weight force exerted by the drone, as mass of the drone is 387.343 kg.

$$\Sigma F = ma$$
$$Ttotal - W = 0$$
$$Ttotal = W$$

To get the maximum take off weight, by the high payload drone, the mass of drone is added with total mass of payload which is 200kg and multiplied by gravitational acceleration, $g = 9.81\ m/s2$

$$W = mg \qquad (\mathbf{4-11})$$
$$W = (387.34 + 200)\ kg \times 9.81\ m/s2$$
$$W = 5{,}761.83\ N$$

Hence, the minimum total thrust must be exerted to hover the drone is 5,761.83N. Next, total thrust is divided by four to get the thrust for single coaxial propulsion, shall be exerted.

$$T = Ttotal \div 4$$
$$T = 1{,}440.46\ N$$

Since the needed thrust to hover is 1,440.46N, thus the minimum rotational speed shall be used for the propeller is 4000 rpm where it will exert 4,843.26N of thrust referring to simulation result previously. Rotational speed of 3000 rpm shall not be used because it only generate 1,424.15N of thrust which is lower compared to the thrust needed to hover the high payload drone.

However, because the thrust generated is significantly greater than its weight, the drone will be lifted with a value of acceleration, based from Equation 4-10.

$$\Sigma F = ma$$
$$Ttotal - W = ma$$
$$(4{,}843.26 \times 4) - 5{,}761.83 = 587.34a$$
$$a = 23.17\ m/s2$$

Overall, the high payload drone is able to take off with 4,000 rpm as rotor power of 68.75 kW for the top rotor and 70.34 kW for the bottom rotor thus producing vertical acceleration of 23.17 $m/s2$.

(b) Take Off and Hovering Requirement

With the intention of identifying the capability of drone to be lifted by the rotational speed configured, resultant forces that acting onto the drone shall be resolved.

According to Newton's second law of motion, the vector sum of the forces, on an object is equal to the mass, of that object multiplied by the acceleration of that object as shown in Equation 4-10.

$$\Sigma F = ma \qquad (\mathbf{4-10})$$

By applying the equation onto the drone and targeting the drone to be hovered in the air, where zero acceleration occurs, thrust generated by the propeller must be equal to the weight force exerted by the drone.

$$\Sigma F = ma$$
$$Ttotal - W = 0$$
$$Ttotal = W$$

Published by FAZ Publishing
http://www.fazpublishing.com/jaat

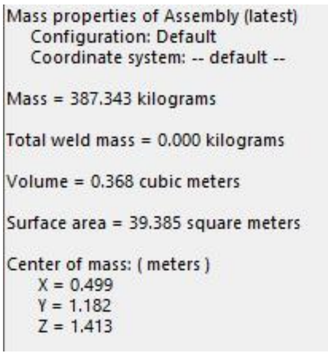

Fig 12- Mass of drone calculated by Solidworks

To get the maximum take-off weight, by the high payload drone, the mass of drone is added with total mass of payload which is 200kg and multiplied by gravitational acceleration, $g = 9.81\ m/s2$

$$W = mg\ (4-11)$$
$$W = (387.34 + 200)\ kg \times 9.81\ m/s2$$
$$W = 5{,}761.83\ N$$

Hence, the minimum total thrust must be exerted to hover the drone is 5,761.83N. Next, total thrust is divided by four to get the thrust for single coaxial propulsion, shall be exerted.

$$T = Ttotal \div 4$$
$$T = 1{,}440.46\ N$$

Since the needed thrust to hover is 1,440.46N, the estimated minimum rotational speed is in between 3000 RPM and 4000 RPM. Hence, the minimum estimated rotational speed calculated based on the equation of trendline extracted from the graph in **Error! Reference source not found.**, where is the minimum thrust value needed by the propeller and is the rotational speed by the propeller.

$$y = 0.0002x2 + 0.1645x - 342.55$$
$$1\,440.46 = 0.0002x2 + 0.1645x - 342.55$$
$$x1 = 2\,602.75\ rpm$$
$$x2 = -3\,425.25\ rpm$$

Correlate with results obtained from the simulation, it was shown that the rotational speed for the propeller should be more than 3000 RPM because this value only produced 1,424.15N of thrust which is lower than minimum thrust needed. Thus, $x2$ which was 3,425.25 RPM is selected as the minimum rotational speed for the drone to hover since $x1$ is lower than 3000 RPM. Negative value of rotational speed can be neglected since it indicates the rotating direction for the propeller.

However, by taking the result directly from simulation, the minimum rotational speed shall be used for the propeller is 4000 rpm where it will exert 4,843.26N of thrust referring to simulation result previously. Rotational speed of 3000 RPM shall not be used because it only generate 1,424.15N of thrust which is lower compared to the thrust needed to hover the high payload drone.

In addition, because the thrust generated is significantly greater than its weight, the drone will be lifted with a certain value of acceleration, a based from Equation 4-10.

$$\Sigma F = ma$$
$$Ttotal - W = ma$$
$$(4{,}843.26 \times 4) - 5{,}761.83 = 587.34a$$
$$a = 23.17\ m/s2$$

Overall, the high payload drone is able to take off with 4,000 rpm producing vertical acceleration of 23.17 $m/s2$. However, this large value of acceleration may be discomfort for the passengers inside the drone. This study is using vertical acceleration by the elevators as reference for the maximum acceleration of the drone to ensure the comfortability of the passengers. According to James Fortune [43], comfortable vertical acceleration shall be ranging from 1.0 $m/s2$ to 1.5 $m/s2$. Thus by targeting maximum acceleration of 1.5 $m/s2$ for the drone, the total thrust shall be produced is calculated as below:

$$\Sigma F = ma$$
$$Ttotal{,}comfort - W = ma$$
$$Ttotal{,}comfort - 5{,}761.83 = 587.34\ (1.5)$$
$$Ttotal{,}comfort = 5{,}849.93\ N$$

With the thrust of 5,849.93N which results in 1.5 $m/s2$ of vertical acceleration, the speed of the drone can be predicted within specific time given.

$$v = u + at$$
$$v = 0 + 1.5\ (5mins \times 60s)$$
$$v = 450\ m/s$$

where v is the speed of the drone, u is the initial speed of drone which was 0 m/s and t is the time where the drone is take off and accelerating

From the calculation, the speed of high payload drone is 450 m/s within 5 minutes of acceleration at 1.5 $m/s2$ with total thrust generation of 5,849.93N by taking human comfortability into consideration.

4.4 Formation of Drag Force in Forward Moving

(a) Drag Coefficient

In this section, the reaction of aerodynamic properties of high payload drone in terms of drag is to be investigated. The simulation conducted for this study was by changing the angle of air trajectory. Data achieved are distributed according to the tilting angle.

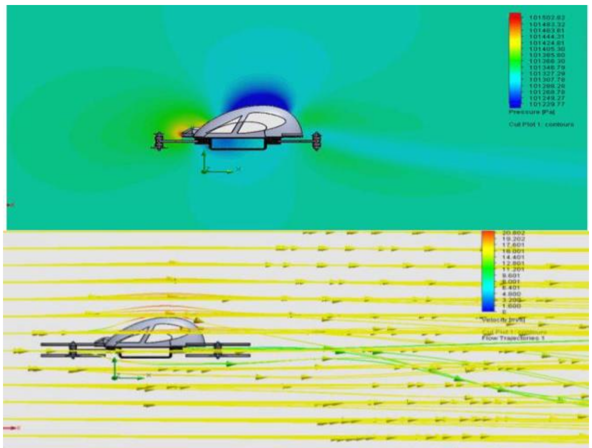

Fig- (a) Tilting angle, α at 0°

Fig-(b) Tilting angle, α at 5°

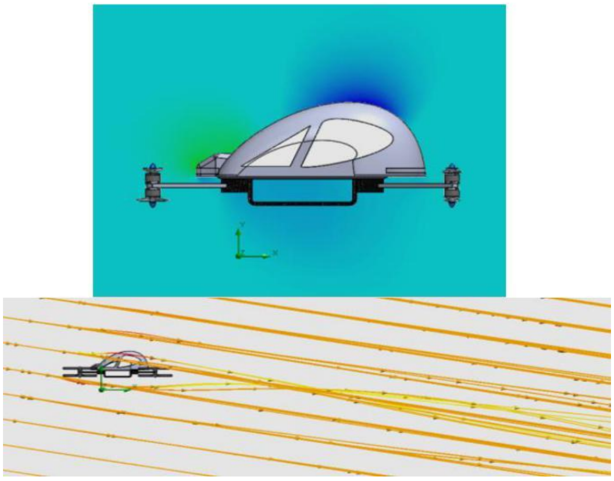

Fig- (c) Tilting angle, α at 10°

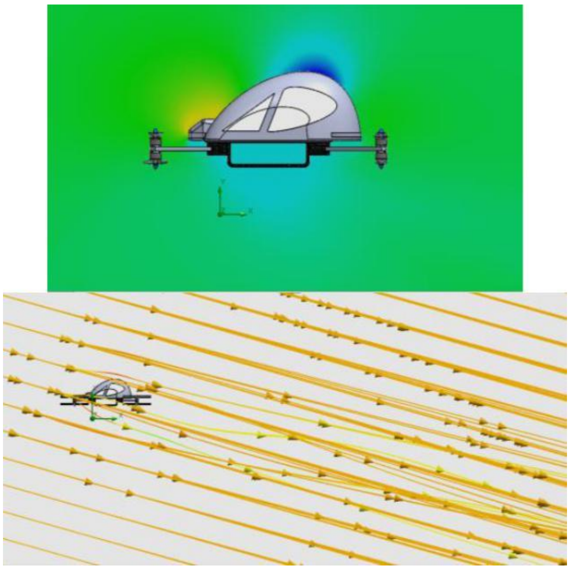

Fig- (d) Tilting angle, α at 15°

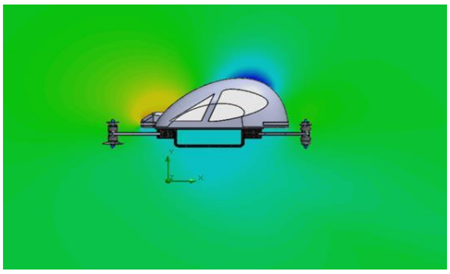

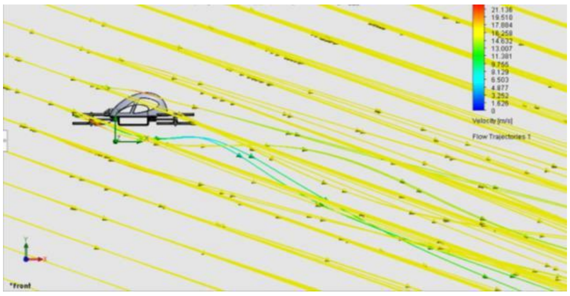

Fig- (e) Tilting angle, α at 20°

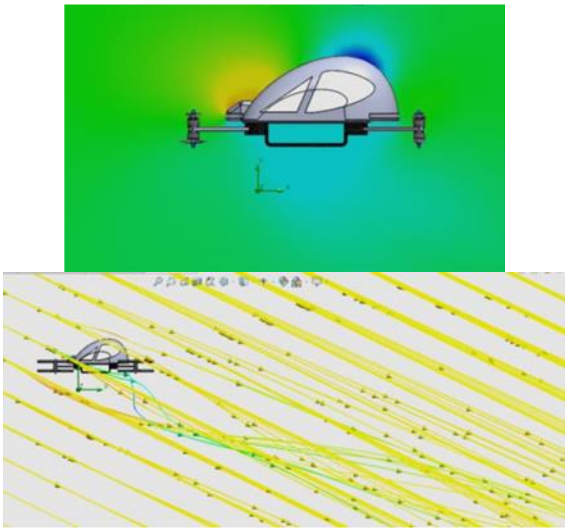

Fig- (f) Tilting angle, α at 25°

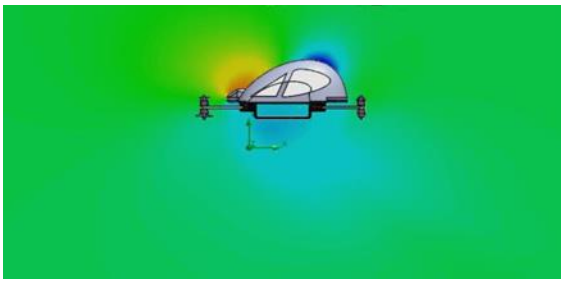

Published by FAZ Publishing
http://www.fazpublishing.com/jaat

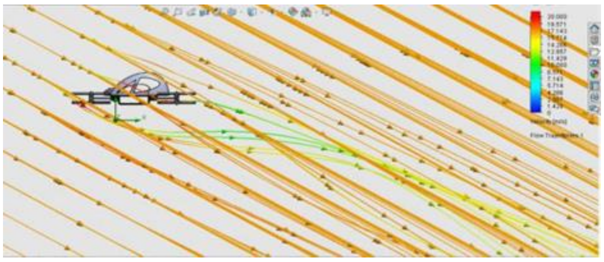

Fig- (g) Tilting angle, α at 30°

Table 9-Result from flow simulation

Angle of air trajectory, (°)	**Drag Coefficient,**
0	0.2978
5	0.3376
10	0.4247
15	0.5679
20	0.7965
25	1.0578
30	1.2964

Angle of air trajectory, α		Drag Force
Degree (°)	Radian	(N)
0	0	215.3370
5	0.0873	244.1046
10	0.1745	307.0971
15	0.2618	410.6961
20	0.3491	575.9745
25	0.4363	764.9812
30	0.5236	937.5257

Table 10- Drag coefficient obtained

Based from the pressure contour obtained, it gave visualization for the motion of the drone as it moves forward passing through the atmosphere. The pressure contour presented showed that the pressure on top of the roof of the body is having the lowest air pressure compared to the rest of the body. This occurrence denotes that the drone shall be tilted to the front as it moves forward across the air.

According from the first simulation conducted where zero degree was setup for the angle of air trajectory and results in tilted motion profile of the drone, hence study in drag forces formed is done by varying the angle of air trajectory.

From the arranged data, a graph of drag coefficient against angle of air trajectory is to be plotted. Several parameters have to be defined with the aim of achieving drag coefficient, CD based from Equation 4-12.

$$C_D = \frac{2D}{\rho A V^2} \quad \textbf{(4-12)}$$

where V is the air velocity at 16.667 m/s, air density, ρ at 1.2 $kgm2/s3$ and reference area, A used is 4.3387 $m2$.

All these parameters were kept constant for each simulation. Table 10 presented the CD obtained while Figure 13 is the plotted graph for the result obtained.

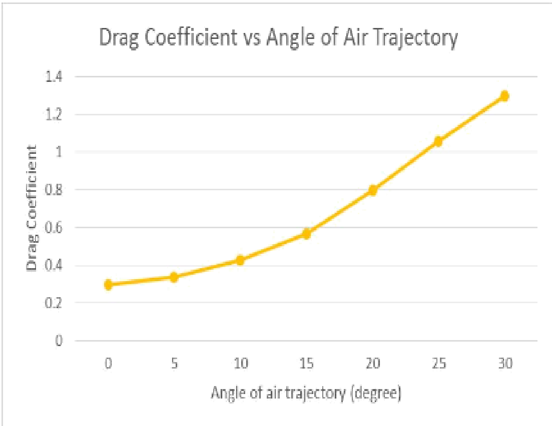

Fig 13- Drag coefficient against angle of air trajectory

Based from the graph in Figure 13, it is visibly shown that as the angle of air trajectory increase, the drag coefficient also increases. If the other parameters is to be kept constant, increased in drag coefficient will results in rises of drag forces. Thus, simultaneously with the result obtained in Table 9, increase in the angle of air trajectory will result in increment of drag forces formed.

(b) Forward Moving of High Payload Drone

Study on forward motion of the drone uses one specified value of total thrust generated by the drone, and resolved this force into x-direction relatively with tilting angle of the drone. By applying Equation 4-10, the acceleration of the high payload drone as it moves forward can be tabulated.

$$Ttotal, comfort - W = ma$$

Table 11- Acceleration obtained as drone moves forward

Tilting angle, (degree)	Thrust in x-direction (N)	Drag (N)	Acceleration, ($m/s2$)
0	0	215.34	-0.37
5	509.85	244.10	0.45
10	1015.83	307.10	1.21
15	1514.07	410.70	1.88
20	2000.79	575.97	2.43
25	2472.29	764.98	2.91

30	2924.96	937.53	3.38

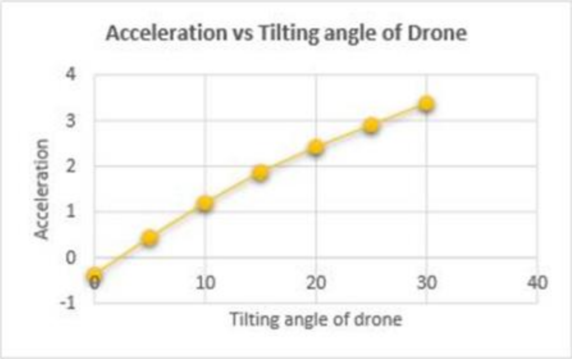

Figure 14-Acceleration of drone against tilting angle of drone

The negative value of acceleration can be ignored since it indicates the deceleration of the high payload drone when it is not tilted to any degree of angle. Next, the velocity of the drone after 5 minutes of constant acceleration is calculated by using kinematic equation, $v = u + at$, and the distance travelled by the drone correlate with its velocity in moving forward is calculated by rearranging equation $v2 = u2 + 2as$, where s is the distance travelled by high payload drone and initial velocity, u is kept zero.

5.0 Summary

This study is conducted by the reason of the growing concept of urban mobility across many countries. An innovative approach for mode of transportation designed for merchandises and societies should be further studied since this urban mobility is able to overcome the complications faced by current available vehicles such as helicopters are used for search and rescue mission where it is a costly task for short time of period.

Because this sort of UAV is still new at this present time, its design prerequisite is yet to be look into alongside with verification of its airworthiness certification. From comparison made, it can be concluded that the proposed design of high payload drone is able to fulfil some of the requirement stated by the certification. However, there are still some aspect to be taken into a count such as material testing, strength, construction, flight characteristics and others. Therefore, the first objective for this research is achieved.

When it comes to vehicle, study of its aerodynamic properties are necessary. Vehicles might not be stable at any great speed and consume more fuel or electricity if it is not well-designed aerodynamically. So, this study investigates the aerodynamic characteristics for proposed design in terms of lift and drag. Based from the simulation results, the suggested design of propeller is able to generate enough thrust to lift the high payload drone which was 4000 rpm producing 4,843.26N of thrust for single coaxial propulsion. However, the minimum thrust needed to hover the high payload drone is just around 1,440.46N thus the rotational speed calculated based on the equation extracted from the trendline is 3,425.25 RPM needed to generate enough thrust. Also, by taking human comfort for the acceleration of the drone, it was calculated that the total thrust needed to be generated is 5,849.93N to result in targeted acceleration of 1.5 $m/s2$. Hence, the second objective of this thesis is reached.

Last but not least, every object that is in motion will produce drag forces. And the last objective for this study is accomplished as it was found that drag forces increases as the tilting angle of drone increases. Subsequently, the value for drag coefficient rises as well as the tilting angle of the drone increases. Although the drag force increases as the tilting angle of drone increases, the horizontal acceleration for the drone also increases when the tilting angle of drone increases.

References

[1] A. Cavoukian, "Privacy and Drones: Unmanned Aerial Vehicles," 2012.
[2] Strict, "Projecteindrapport v1.0," 2016.
[3] Uber Elevate, "Fast-Forwarding to a Future of On-Demand Urban Air Transportation," pp. 1–98, 2016.
[4] C. P. Coleman, "A Survey of Theoretical and Experimental Coaxial Rotor Aerodynamic Research," 1997
[5] H. W. Kim and R. E. Brown, "A Comparison of Coaxial and Conventional Rotor Performance," *J. Am. HELICOPTER Soc.*, vol. 55, 2010.
[6] R. Online, L. Chen, P. J. Mckerrow, L. Chen, and P. Mckerrow, "Modelling the Lama Coaxial Helicopter Modelling the Lama Coaxial Helicopter Modelling the Lama Coaxial Helicopter," pp. 1–9, 2007.
[7] C. M. Simões, "Optimizing a Coaxial Propulsion System to a Quadcopter," pp. 1–10, 2015.

Published by FAZ Publishing
http://www.fazpublishing.com/jaat